Journal of Thermal Analysis and Calorimetry, Vol. 61 (2000) 565–578

STUDY OF THE CRYSTALLIZATION OF AN AROMATIC POLY-ETHER-KETONE (PK99) BY CALORIMETRIC AND X-RAY ANALYSIS

L. Torre[1], *J. M. Kenny*[1], *A. Recca*[2], *V. Siracusa*[2], *A. Tarzia*[3] *and A. Maffezzoli*[3*]

[1]Istituto di Tecnologie Chimiche, Università di Perugia, Terni
[2]Istituto Chimico, Facoltà di Ingegneria Università di Catania
[3]Dipartimento di Ingegneria dell'Innovazione, Università di Lecce, Via Arnesano, 73100, Italy

Abstract

An analysis of the crystallization behaviour of a new poly(aryl-ether-ether-ketone-ketone), PK99, by differential scanning calorimetry (DSC) and wide-angle X-ray diffraction (WAXD) is presented. Isothermal crystallization TG were obtained in the whole range between the glass transition temperature (T_g) and the melting temperature (T_m) as a consequence of the slow crystallization kinetics stemming from the closeness of these transitions. The calorimetric results, compared with WAXD data, were applied to determine the theoretical melting temperature and crystallization enthalpy. The DSC and WAXD data were combined in order to calculate the total amount of the crystallizable fraction of the polymer, and a model was proposed to explain the difference between the fractions of crystallinity observed with these techniques. The thermal and X-ray data were also correlated with different lamellar morphologies arising from the crystallization conditions. Finally, DSC experiments on the crystallized sample were used to detect the presence of a rigid amorphous phase which does not relax at T_g.

Keywords: crystallization, DSC, PK99, rigid amorphous fraction, WAXD

Introduction

Since their introduction, engineering thermoplastics of the family of aromatic ether-ketone polymers have generated considerable interest, mainly in the aerospace industry, as the leading matrix candidates for use in advanced composites. More recently, these polymers have been used in load-bearing applications in their injection molding grades, usually reinforced with short fibers. Their attractive properties are essentially related with their high continuous service temperatures, coupled with an elevated yield strength. Extensive research is mainly available on poly(ether-ether-ketone) (PEEK), the most widely diffused in this family [1, 2].

* Author for correspondence: e-mail: maffez@axpmat.unile.it

1418–2874/2000/ $ 5.00
Akadémiai Kiadó, Budapest

A new polymer belonging among the aryl-ether-ketones has recently been synthesized: poly(aryl-ether-ether-ketone-ketone) (PK99) [3]. This polymer is characterized by a glass transition temperature (T_g) of about 160°C, higher than the T_g of PEEK, and a melting point (T_m) of the main crystallites of 300°C, a temperature lower than the T_m of PEEK. These transitions allow lower processing temperatures and lower cooling rates to quench the polymer in the amorphous state. Furthermore, thermal degradation studies on PK99 [3] have shown that this polymer presents a better thermal stability than that of PEEK.

The study of the crystallization processes is very important for the characterization of thermoplastic polymers, since most of the main properties are related to their morphology. The determination of the processing conditions in terms of cooling rates and mold temperature is strictly related to the crystallization kinetics, and some physical and mechanical properties, such as the environmental stability, the solvent resistance and the modulus, depend strongly on the crystallinity content of the polymer [4].

In order to obtain a complete characterization of the crystallization behaviour, it is necessary to determine some intrinsic properties of the polymer, such as the theoretical equilibrium melting temperature T_m^0 and the heat of crystallization of the pure crystals. These values are usually obtained by using X-ray data combined with calorimetric analysis. The determined degree of crystallinity, either in mass or in volume, obtained from wide-angle X-ray diffractometry (WAXD) or enthalpy measurements, is not an accurate measure of the fraction of polymer that is not amorphous, i.e. 'liquid-like'. The crystal fractions obtained by using these two techniques are usually different, depending on the different natures of the measurements and on the attribution of the chain-folded matter at lamellar surfaces either to the crystalline or to the amorphous phase. This intrinsic inaccuracy is essentially related with the chain-folded morphology of most of the bulk-crystallized polymers. In particular, the crystal surfaces represent an energy-rich region of the lamellar crystals that can be considered either part of the crystalline phase of the polymer or part of the amorphous phase.

Moreover, the crystal morphology strongly affects the molecular mobility of the amorphous phase. Depending on the crystal nucleation, growth and morphology, the number of amorphous chains, which are 'trapped' between crystals, and therefore behave as rigid chains, can vary significantly. Several semicrystalline polymers show the presence of these amorphous immobilized chains, which do not relax at T_g [5] and could affect some of their mechanical and physical properties. The amount of the rigid amorphous phase can be determined by analyzing the variation in the heat capacity (C_p) in relation to T_g, this variation depending on the contribution of the amorphous chains which are not immobilized in the crystals. By means of calorimetric analysis, this fraction can be calculated as follows:

$$X_{ma} = \frac{\Delta C_{pc}}{\Delta C_{pa}} \quad \text{and} \quad X_{mra} = 1 - X_{ma} - X_{mc} \tag{1}$$

where X_{ma} and X_{mra} are the total amorphous and rigid amorphous mass fractions, X_{mc} is the mass fraction of crystallinity, and ΔC_{pc} and ΔC_{pa} are the variations in the specific

heat at T_g of the amorphous and the semicrystalline polymer. Such values can be related with the crystallization temperature and the different crystalline fractions obtained from X-ray and DSC.

This work presents a preliminary characterization of the crystallization behaviour of PK99, using DSC and WAXD. The main properties of this polymer have been calculated and analyzed, in order to provide information and a database for a kinetic analysis of the crystallization of PK99. Furthermore, the data have been analyzed on the hypothesis that the amount of chain-folded crystalline matter (considering the crystals to consist of bulk and surfaces) developed during melt crystallization is not a function of the undercooling. The significantly lower values of the degree of crystallinity calculated by DSC as compared with WAXD measurements have been interpreted in terms of the polymer fraction belonging to the chain-folded surfaces.

Experimental

Materials

The PK99 used in this work was synthesized by ICI [6]. Its structural formula is reported in Fig. 1. Polymer pellets for DSC and WAXD characterizations were dried in a vacuum oven.

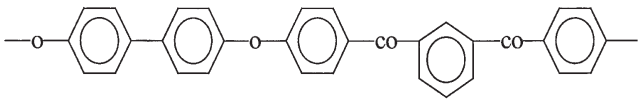

Fig. 1 Structural formula of PK99

Equipment and procedures

DSC was performed with a Perkin Elmer DSC Pyris 1 instrument equipped with a Perkin Elmer Intracooler 2 as cooling equipment. This can operate from –60 to 550°C, allowing cooling rates up to 150°C min^{-1}. DSC tests were performed in both isothermal and non-isothermal modes. Isothermal melt crystallization experiments were performed with the polymer kept at 320°C for 5 min and then cooled down at 100°C min^{-1} to the crystallization temperature, which ranged from 245 to 280°C in 5°C steps. After each isothermal test, part of the material was analyzed by WAXD and the remaining part was heated in a DSC temperature scan at 20°C min^{-1}.

WAXD was performed by using a standard XRD-Philips instrument equipped with a CuK_α source. Diffraction patterns were collected on samples obtained from crystallization performed in the DSC pan.

Results and discussion

Calorimetric analysis

Figure 2 depicts a dynamic scan at 20°C min^{-1} on a dried sample. The polymer shows a glass transition temperature of 160°C. A small melting peak (almost 10% of the total crystallization heat), characterized by an onset around 215°C and related to low-temperature melting crystals, is then observed. An additional cold crystallization peak, with onset at 245°C, is followed by crystal melting occurring between 280 and 320°C. Integration of the melting peak provides a heat of fusion of 39 J g^{-1}.

The presence of a low-melting phase is observed better in Fig. 3, which features a non-isothermal scan performed after a cold crystallization test at 220°C. At this temperature, in fact, only the low-melting phase crystallizes, and the resulting dy-

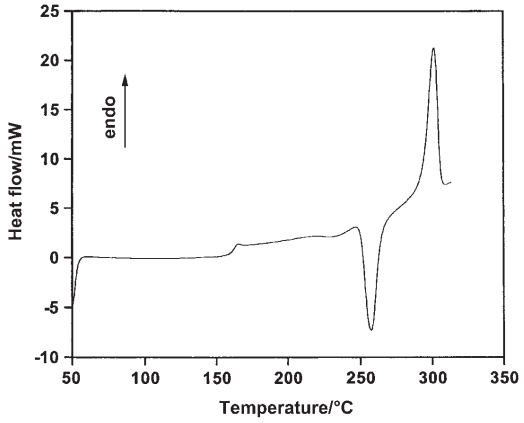

Fig. 2 Non-isothermal DSC scan at 20°C min^{-1} on the as-received sample

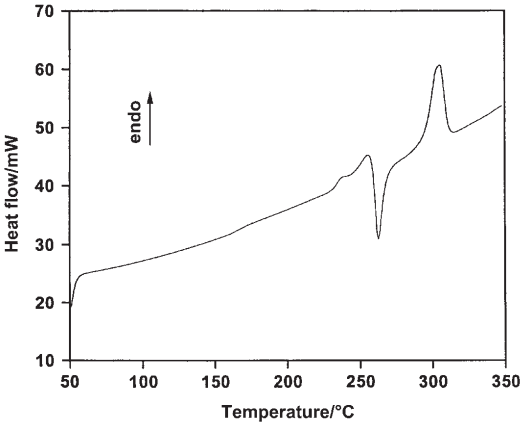

Fig. 3 Non-isothermal DSC scan at 20°C min^{-1} on a sample cold-crystallized at 220°C

namic scan presents an endothermic peak at about 220°C, related to the melting of this phase, followed by a strong additional crystallization peak at 250°C.

Cooling experiments were performed in order to identify the processing window of PK99. In order to melt the crystals completely, the polymer was held at 320°C for 5 min and then cooled down to room temperature at different cooling rates (from 50 to 5°C min^{-1}). A dynamic scan from room temperature up to the molten state was then performed. The relative amount of crystallinity (X_{mcrel}) developed during the former cooling DSC experiment was calculated by comparing the heat of additional crystallization observed when the sample was heated above T_g. ΔH_{ac}, and the heat of fusion of the crystals, ΔH_m:

$$X_{mcrel} = 1 - \frac{\Delta H_{ac}}{\Delta H_m} \quad (2)$$

The characteristic narrow processing window of this polymer is clearly shown in Fig. 4, where X_{mcrel} is plotted as a function of the cooling rate. This reveals the slow crystallization kinetics of PK99: a cooling rate of 30°C min^{-1} yields an almost amorphous polymer, while a cooling rate of 50°C min^{-1} is needed. in order to quench the polymer completely.

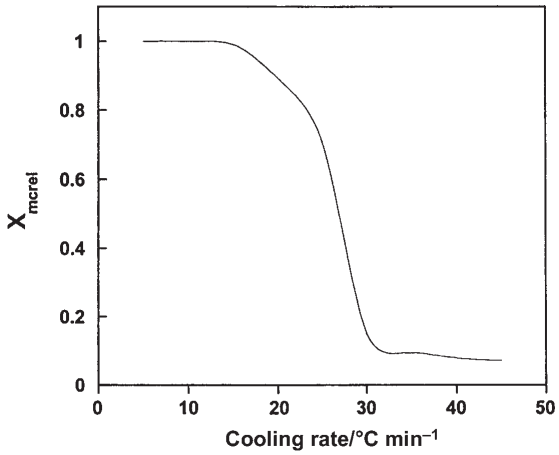

Fig. 4 Effects of different cooling rates on relative crystallinity

The heat of crystallization obtained from melt crystallization experiments is reported for each crystallization temperature in Table 1. After each melt crystallization, a temperature scan was performed in order to evaluate the change in the specific heat at T_8 and the melting temperature T_m. The characteristic double melting peak was always observed and the lower T_m values were used to calculate the theoretical melting temperature [7].

Table 1 Crystallization data obtained from DSC and WAXD

Temperature/°C	ΔH/J g^{-1}	X_{mcWAXD}	X_{mcDSC}	X_{mra}
245	35.1	0.291	0.253	0.40533
250	33.6	0.302	0.243	0.37521
255	34.5	0.303	0.249	0.34712
265	38.6	0.323	0.279	0.34031
270	40.7	0.333	0.294	0.33272
275	41.0	0.328	0.296	0.34634
280	42.0	0.333	0.303	0.36362

The theoretical melting temperature T_m^0 is defined as the melting temperature of an ideal crystal of virtually 'infinite' thickness, characterized by crystallization and melting processes occurring at the same temperature. Therefore, the line $T_m=T_c$ in the plot of T_m as a function of the crystallization temperature (T_c), shown in Fig. 5, represents the lower limit of the melting behaviour. The intercept between this line and the extrapolated experimental data represents the theoretical melting temperature, calculated for PK99 to be 344°C.

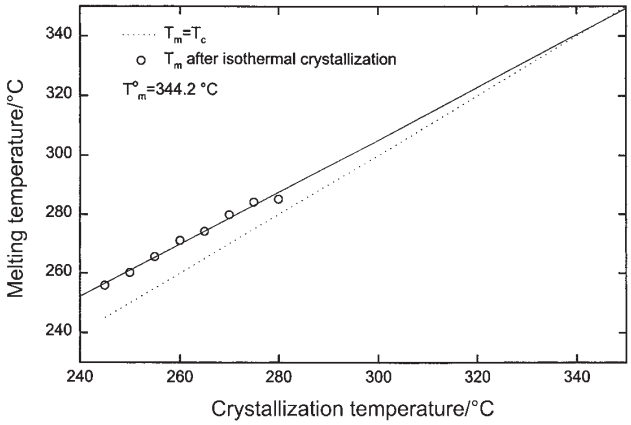

Fig. 5 Hoffman–Weeks plot for the calculation of T_m^0

Analysis of WAXD data

The WAXD diffraction patterns obtained on the same samples isothermally crystallized from the melt in the DSC experiments are compared in Fig. 6. Very similar behaviour is observed for each crystallization temperature. The diffraction patterns of other aromatic poly-ether-ketones strictly resemble those in Fig. 6. This similarity, widely recognized in the literature for this class of polymers [8, 9], leads to the attribution of the crystalline planes indicated in Fig. 6. In particular, as pointed out by

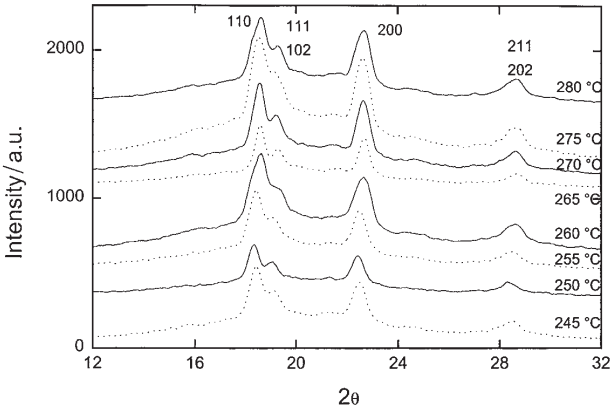

Fig. 6 WAXD diffraction patterns obtained on samples crystallized from the melt at different temperatures

Rueda *et al*. [10] in the case of polyketones crystallized from the melt, orthorhombic packing is always observed for all polyketones, regardless of their carbonyl content.

The 200 reflection may be used to measure the lattice parameter *a* of the unit cell, and this value may be compared with those of other poly-ether-ketones. The lattice parameter *a*, reported by Blundell and Newton [11] for polymers of the general formula [–Ar–X–], where *X* is a ketone or an ether linkage, is compared with that of PK99 in Table 2.

Table 2 Lattice parameters *a* for some aromatic poly-ether-ketone polymers

	PPO	PEEK	PEK	PEEKK	PK99	PEKEKK	PEKK
a [1, 12]	0.803	0.786	0.776	0.780	0.794	0.774	0.769 [9]
Ketone%	0	33	50	50	50	60	66

PPO (poly-phenylene-oxide); PEEK (poly-ether-ether-ketone); PEK (poly-ether-ketone); PEEKK (poly-ether-ether-ketone-ketone); PEKEKK (poly-ether-ketone-ether-ether-ketone); PEKK (poly-ether-ketone-ketone)

As shown in this Table, the link between two aromatic rings in PK99 significantly changes this lattice parameter with respect to other polymers characterized by the same ratio between the ether and ketone groups. Conversely, as noted by Blundell and Newton [11], poly-ether-ketone (PEK) and poly-ether-ether-ketone-ketone (PEEKK) are characterized by very similar crystalline unit cells. It can also be noted that PK99 presents the highest value of parameter *a*, while a monotonous decrease with the ketone content is observed for the other polymers [10].

The diffraction peaks labelled 211 and 202 (about 28.6°) can be used to obtain an indication of the crystal dimensions in a direction that should be significantly affected by the different lamellar thicknesses arising at different crystallization temperatures. The peak area, A_m, was calculated after converting the abscissa 2θ in units of

s=2sinθ/λ (λ=wavelength). The effect of a different sample mass, w, was taken into account by normalizing each measured area, A_m, as follows:

$$A_n = A_m \frac{w_{max}}{w} \tag{3}$$

where A_n is a normalized value and w_{max} is the maximum mass among the tested samples.

The temperature dependence of the parameter A_n, shown in Fig. 7, indicates that, as expected, larger crystals and thicker lamellae develop at higher crystallization temperatures.

The volume fraction of crystallinity calculated by means of WAXD (X_{vcWAXD}) was estimated from the ratio of the integrated intensity of peaks associated with crys-

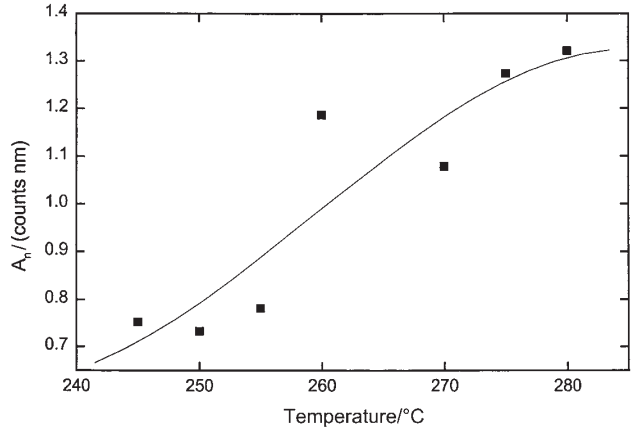

Fig. 7 Normalized area of the peak at 28.6° as a function of the crystallization temperature

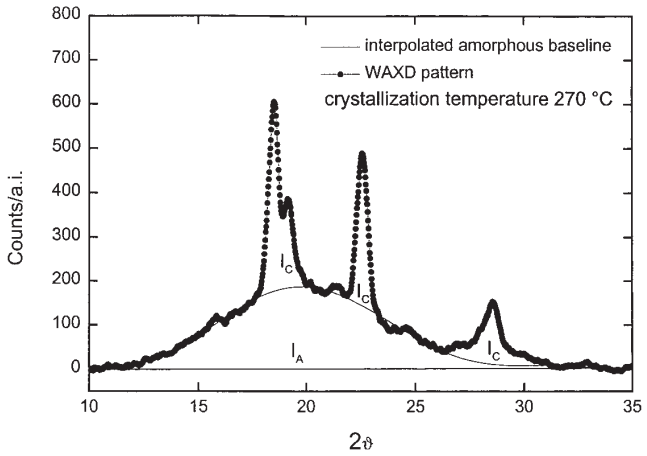

Fig. 8 Calculation procedure for X_{vcWAXD} for a WAXD curve on a sample crystallized at 270°C

talline reflections (I_C) to the total integrated area of the spectrum, given by the sum of the amorphous (I_A) and crystalline contributions [13], i.e.

$$X_{\text{vcWAXD}} = \frac{I_C}{I_C + I_A} \tag{4}$$

The indicated areas are shown in Fig. 8 for a sample crystallized from the melt at 270°C in the DSC. The values obtained from Eq. (4), converted to mass fraction of crystallinity by using the densities of the amorphous and crystalline phases, are listed in Table 1.

Comparison between DSC and WAXD data

The mass fraction of crystallinity, obtained from the X_{vcWAXD} data, is combined with the heat of crystallization reported in Table 1, leading to a heat of melting of the full crystalline polymer ΔH_0=119.9±5.4 J g^{-1}. This value is comparable with that reported in the literature for PEEK (130 J g^{-1}) [12].

The mass fraction of crystallinity (X_{mcDSC}) was calculated from DSC isothermal crystallization experiments as the ratio between the isothermal heat of crystallization of a sample (ΔH_C) [14–25]:

$$X_{\text{mcDSC}} = \frac{\Delta H_C}{\Delta H_0} \tag{5}$$

ΔH_0 is a reference value corresponding to the heat of crystallization of a crystal of infinite lamellar thickness characterized by a melting temperature, T_m^0 significantly higher than that observed in a DSC heating scan on a bulk-crystallized polymer.

As highlighted by Hoffman *et al*. [7], the determined degree of crystallinity, in mass or in volume, obtained from WAXD, density or enthalpy measurements, is not an accurate measure of the fraction of polymer that is not 'liquid-like'. This intrinsic inaccuracy is essentially related with the chain-folded morphology of most of the bulk-crystallized polymers. In particular, the crystal surfaces represent energy-rich regions of the crystalline phase that can be considered a portion of the crystalline phase of the polymer. The enthalpy content of a lamellar crystal may be regarded as the sum of the exothermic contribution of the bulk portion and the endothermic contribution of the chain-folded and the lateral surfaces. The energetic contribution of the lateral surfaces of the crystal is usually 5–10 times lower than that the fold surfaces. Furthermore, the lateral surfaces are characterized by an area significantly lower than that of the fold surfaces as a consequence of the typical flat morphology of lamellar crystals. The rougher the fold surface of a lamellar crystal, the lower the apparent heat of crystallization of the crystal, properly considered as consisting of bulk and surfaces [7]. Consequently, the heat of crystallization measured in an isothermal DSC experiment can be considered to be the sum of two contributions:

1. an exothermic crystallization enthalpy associated with the formation of the bulk portion of the crystals;

2. an endothermic enthalpy contribution associated either with the work of chain folding required for the formation of fold surfaces or with the extent of roughness of this surface.

Therefore, it may be concluded that the heat of crystallization measured by DSC is a function of the aspect ratio of the lamellar crystals. The experimental evidence indicates that the thickness of a lamellar crystal increases as the crystallization temperature increases up to the theoretical melting temperature T_m^0, where an ideal infinite lamellar thickness should be obtained. The increase in the degree of crystallinity, obtained by enthalpy measurements, with the undercooling can therefore be interpreted in accordance with the former considerations.

It must be noted that the isothermal heat of crystallization is measured during the crystal growth, while WAXD experiments are usually performed at room temperature, when the crystalline phase is already completely developed. The contribution of the fold surface to the degree of crystallinity observed by WAXD is definitely negligible. On the other hand, the enthalpy measurements are the result of a balance between the positive contribution by the energy content of the fold surfaces and the negative contribution by the latent heat of crystallization. These considerations can explain why the values of X_{mcDSC} are always lower than X_{mcWAXD} (Table 1).

The hypothesis on which this analysis of the data is based is that the amount of chain-folded crystalline matter (the crystals being taken to consist of bulk and surfaces) developed during a cold or melt crystallization is not a function of the undercooling. This assumption may be qualitatively justified if it is considered that the amount of non-crystallizable material should not increase if the crystallization temperature is decreased. In other words, a significant decrease in the degree of crystallinity, as calculated by means of DSC measurements in accordance with a higher degree of undercooling, would imply that at lower temperatures the amount of non-crystallizable chain segments is increased [15]. The assumption in this work of a constant amount of crystallizable matter justifies a reduction of the enthalpy content

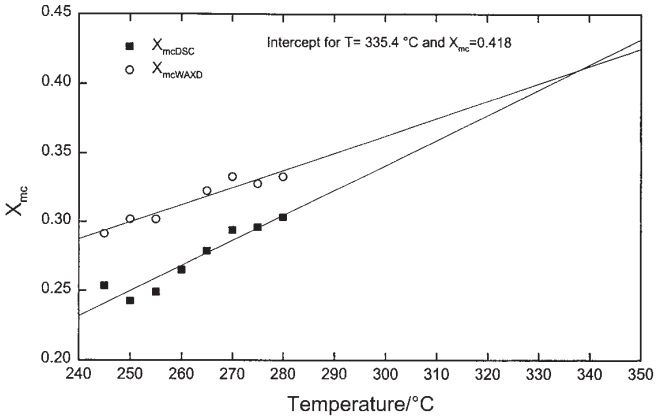

Fig. 9 Temperature dependences of X_{mcDSC} and X_{mcWAXD}

of the crystals grown at increasing undercooling in terms of different morphologies, rather than in terms of different degrees of crystallinity.

X_{mcDSC} and X_{mcWAXD} exhibit temperature dependences characterized by different slopes, as reported in Fig. 9. Linear extrapolation of the apparent trends of the two sets of data leads to an intercept at a maximum value of the mass fraction of crystallinity, X_{mcmax}=0.418, which can be regarded as the maximum amount of chain-folded crystallizable matter available in the PK99 studied. Moreover, the extrapolated X_{mcmax} is situated at a temperature (335°C) only slightly lower than the T_m^0 calculated from the Hoffman–Weeks plot in Fig. 5. The difference between X_{mcDSC} and X_{mcWAXD} should become negligible in accordance with a theoretical crystallization temperature at which very thick lamellar crystals can grow the contribution of the fold surfaces being negligible for such crystals. This temperature should be close to T_m^0, where crystals of infinite thickness form and melt. Although this result has been obtained by introducing the strong approximation of a linear temperature dependence of X_{mcDSC} and X_{mcWAXD}, it provides further support for the hypothesis of a constant level of crystallizable matter. The same results were reported in an earlier paper [26] on the crystallization of a new thermoplastic polyimide. In this paper, an enthalpy balance on a chain-folded crystal was applied to explain the temperature dependence of the heat of crystallization measured by DSC, using a constant value of the mass fraction of crystallinity and hence assuming a constant amount of crystallizable matter.

The simple linear extrapolation in Fig. 9 can be improved by using an accepted expression for the temperature dependence of the lamellar thickness, l [27]:

$$l=C_1+\frac{C_2}{\Delta T} \tag{6}$$

where C_1 and C_2 are fitting parameters and ΔT is the undercooling, T_m^0-T.

On the basis of the discussion presented above, X_{mcWAXD} may be considered to be essentially dependent on the aspect ratio of the crystals. When this aspect ratio (given by the lamellar thickness for prismatic crystal geometry) for ΔT=0 goes to infinity, X_{mcWAXD} attains its maximum value. The following expression may therefore be reasonably adopted

$$X_{mcWAXD}=P_1-\frac{P_2}{l} \tag{7}$$

where P_1 and P_2 are fitting parameters.

From a combination of the last two equations, the temperature dependence of X_{mcWAXD} can be expressed as

$$X_{mcWAXD}=P_1-\frac{P_2\Delta T}{C_1-\frac{C_2}{\Delta T}} \tag{8}$$

This four-parameter expression is fitted to the experimental data (the same as reported in Fig. 9), imposing the value of T_m^0 calculated from the Hoffman–Weeks plot

(Fig. 5). The fitting of Eq. (8) to the X_{mcWAXD} data is shown in Fig. 10, with P_1=0.364, P_2=0.1294°C^{-1}, C_1= –3.09 and C_2=476.9°C obtained from non-linear regression analysis. In this case, a more reliable value of $P_1=X_{mcmax}$=0.364 has been predicted at T_m^0. This value can be taken as the maximum amount of crystallizable matter in the studied grade of PK99.

This result may be further exploited in order to calculate the amount of chain segments that are part of lamellar crystals as chain-folded matter. This polymer fraction, not detected by WAXD, contributes with the endothermic heat of chain folding to the enthalpy of crystallization measured in isothermal DSC experiments. If the energy content of the lateral surfaces of a chain-folded crystal is negligible, the endo-

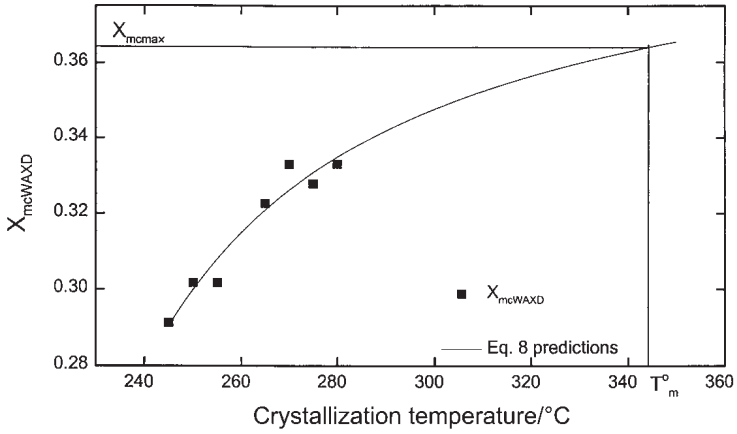

Fig. 10 Comparison of X_{mcWAXD} data and Eq. 8 predictions

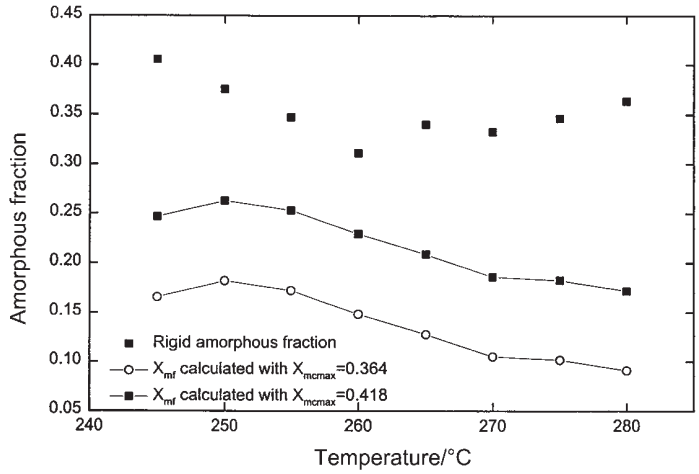

Fig. 11 Comparison between the rigid amorphous fraction and X_{mf} calculated by using X_{mcmax}=0.418 and X_{mcmax}=0.364

thermic contribution of chain folding to the heat of crystallization (Δq) can be computed as

$$\Delta q = \Delta H_0 \, (X_{\text{mcmax}} - X_{\text{mcDSC}}) \tag{9}$$

The polymer fraction included in the chain-folded surfaces (X_{mf}) may then be obtained once the work of chain folding, q, is known. Although q is not known for PK99, it can be assumed to be of the same order of magnitude as that calculated for PEEK by Chen and Chung [28]. They calculated q values of 8.2 and 10.1 kcal mol^{-1} for regimes III and II, respectively. If an average value of q=9 kcal mol^{-1} is assumed for PK99, the polymer fraction included in the chain-folded surfaces, $X_{\text{mf}}=\Delta q/q$, can be computed from Eq. (9), using for X_{mcmax} either 0.364 from Fig. 10 or 0.418 from Fig. 9.

The comparison between the rigid amorphous fraction, X_{mra}, and X_{mf}, reported in Fig. 11, suggests that X_{mra} is not simply given from the polymer chains belonging to the chain-folded surfaces of the crystals. However, one source of error is a direct consequence of the procedure used for the calculation of ΔH_0, obtained by attributing the heat of crystallization obtained from DSC to a mass fraction of crystallinity measured by WAXD. As pointed out above, the crystallization enthalpy measured by DSC results from the balance of an exothermic contribution arising from the bulk of the crystal and an endothermic contribution associated with the formation of the chain-folded surfaces. On the other hand, WAXD diffraction patterns result only from the bulk of the lamellar crystals. Therefore, a different value of ΔH_0 could be calculated, accounting for the contribution of Δq to the heat of crystallization measured by DSC. A new value of Δq would then be obtained from Eq. (9), leading to an iterative procedure to estimate ΔH_0.

Nevertheless, although the absolute values of X_{mf} shown in Fig. 11 may be affected by significant errors arising from an oversimplification of the crystal morphology and from the assumption of the value for q calculated for PEEK, there is enough support to conclude that the rigid amorphous behaviour is displayed not only by chain-folded segments at the lamellar crystal surfaces, but also by segments immobilized between crystals.

Conclusions

A preliminary characterization of the crystallization behaviour of PK99 has been proposed, using DSC and WAXD. The main properties of this polymer have been calculated and analyzed, in order to provide a first database for the kinetic analysis of the crystallization of PK99. Furthermore, a constant amount of chain-folded crystalline matter (with the crystals taken to consist of bulk and surfaces) developed during melt crystallization has been assumed for the analysis of data. This hypothesis has led to different maximum mass fractions of crystallinity, depending on the extrapolation procedure applied. The significantly lower values of the degree of crystallinity calculated by means of DSC as compared with WAXD measurements have been interpreted in terms of different amounts of polymer in chain-folded surfaces. Finally, a

comparison has been proposed between the measured rigid amorphous fraction and the calculated amount of polymer in the chain-folded surfaces.

* * *

We thank the Italian MURST for co-financing this research work (Progetto Nazionale: Sistemi Polimerici per Materiali Compositi). The authors are also grateful to Mr. Donato Cannoletta for WAXD measurements.

References

1 D. J. Blundell and B. N. Osborn, Polymer, 24 (1983) 953.
2 P. Cebe and S. D. Hong, Polymer, 27 (1986) 1183.
3 L. Abate, S. Calanna, A. Pollicino and A. Recca, Pol. Eng. Sci., 36 (1996) 1782.
4 J. M. Kenny, L. Torre, L. Nicolais, M. Iannone and C. Voto, Proceedings of SAMPE 13th European Chapter Conference, Basilea 1992, p. 105.
5 S. Iannace and L. Nicolais, J. Appl. Polym. Sci., 64 (1997) 911.
6 P. A. Staniland, Bull. Chem. Soc. Chim. Belg., 98 (1989) 667.
7 J. D. Hoffman, G. T. Davis and J. I. Lauritzen, in Treatise on Solid State Chemistry, N. B. Hannay (ed.), Plenum Press, New York, Vol. 3. chap. 7, 1976.
8 Dawson and D. J. Blundell, Polymer, 21 (1980) 577.
9 K. H. Gardner, B. S. Hsiao and K. L. Faron, Polymer, 35 (1994) 1191.
10 D. R. Rueda, M. G. Zolotukhin, M. E. Cagiao, F. J. Balta Calleja, D. Villers and M. Dosiere, Macromolecules, 29 (1996) 7016.
11 D. J. Blundell and A. B. Newton, Polymer, 32 (1991) 308.
12 D. J. Blundell and B. N. Osborn, Polymer, 32 (1991) 2691.
13 B. Wunderlich, Macromolecular Physics, Vol. 1, Academic Press, New York 1976.
14 L. Torre, A. M. Maffezzoli and J. M. Kenny, J. Appl. Polym. Sci., 56 (1995) 985.
15 N. A. Mehl and L. Rebenfeld, Pol. Eng. Sci., 32 (1992) 1451.
16 S. A. Jabarin, J. Appl. Polym. Sci., 34 (1987) 85.
17 M. Okamoto, Y. Shinoda, N. Kinami and T. Okuyama, J. Appl. Polym. Sci., 57 (1995) 1055.
18 M. R. Kamal and E. Chu, Polym. Eng. Sci., 23 (1983) 27.
19 G. P. Desio and L. Rebenfeld, J. Appl. Polym. Sci., 39 (1990) 825.
20 K. C. Cole, D. Noel, J. J. Hechler and D. Wilson, J. Appl. Polym. Sci., 39 (1990) 1887.
21 P. P. Huo, J. B. Friler and P. Cebe, Polymer, 34 (1993) 4387.
22 S. X. Lu, P. Cebe and M. Capel, J. Appl. Polym. Sci., 57 (1995) 1359.
23 J. Mijovic and T. C. Gsell, SAMPE Quarterly, 42 January (1990).
24 J. M. Kenny, A. Maffezzoli and L. Nicolais, Thermochim. Acta, 227 (1993) 83.
25 J. M. Kenny and A. Maffezzoli, Polym. Eng. Sci., 31 (1991) 607.
26 A. Maffezzoli, L. Torre and J. M. Kenny, J. Appl. Polym. Sci., 67 (1998) 763.
27 B. Wunderlich, Macromolecular Physics, Vol. 2, Academic Press, New York 1976.
28 M. Chen and C. Chung, J. Polym. Sci.: Part B: Polym. Phys., 36 (1998) 2393.